

Poly(vinyl chloride) Hollow-Fiber Membranes for Ultrafiltration Applications: Effects of the Internal Coagulant Composition

Qusay F. Alsalhy,¹ Khalid T. Rashid,¹ Wallaã A. Noori,¹ S. Simone,² A. Figoli,² E. Drioli^{2,3}

¹School of Chemical Engineering, Oil and Gas Refinery Engineering Department, University of Technology, Alsinaa Street No. 52, B. O. 35010, Baghdad, Iraq

²Institute on Membrane Technology, National Research Council, c/o University of Calabria, Via P. Bucci Cubo 17/C, 87030, Rende (Cosanza), Italy

³Department of Chemical Engineering and Materials, University of Calabria, Via P. Bucci Cubo 42/A, 87030, Rende (Cosanza), Italy

Received 12 February 2011; accepted 4 July 2011

DOI 10.1002/app.35220

Published online 26 October 2011 in Wiley Online Library (wileyonlinelibrary.com).

ABSTRACT: Poly(vinyl chloride) (PVC) hollow-fiber membranes were spun by a dry/wet phase-inversion technique from dopes containing 15 wt % PVC to achieve membranes with different pore sizes for ultrafiltration (UF) applications. The effects of the *N,N*-dimethylacetamide (DMAc) concentration in the internal coagulant on the structural morphology, separation performance, and mechanical properties of the produced PVC hollow fibers were investigated. The PVC membranes were characterized by scanning electron microscopy, average pore size, pore size distribution, void volume fraction measurements, and solubility parameter difference. Moreover, the UF experiments were conducted with pure water and aqueous solutions of poly(vinyl pyrrolidone) as feeds. The mechanical properties of the PVC hollow-fiber membranes were

discussed in terms of the tensile strength and Young's modulus. It was found that the PVC membrane morphology changed from thin, fingerlike macrovoids at the inner edge to fully spongelike structure with DMAc concentration in the internal coagulant. The effective pores showed a wide distribution, between 0.2 and 1.1 μm , for the membranes prepared with H_2O as the internal coagulant and a narrow distribution, between 0.114 and 0.135 μm , with 50 wt % DMAc. The results illustrate that the difference in the membrane performances was dependent on the DMAc concentration. © 2011 Wiley Periodicals, Inc. *J Appl Polym Sci* 124: 2087–2099, 2012

Key words: membranes; morphology; phase separation; poly(vinyl chloride) (PVC)

INTRODUCTION

The preparation of hollow-fiber membranes involves many different variables, such as the structure and dimension of the spinneret, the composition and flow rate of the internal coagulant, the polymer dope viscosity, the fiber windup speed, and the air-gap distance. Furthermore, by changing one or more of these variables, which are dependent on each other, one may affect the membrane structure and performance quite significantly. The composition of the internal coagulant is one of the most important parameters affecting the membrane morphology and separation performance.¹

In previous studies, the effect of the internal coagulant composition on the performance of the hollow-fiber membranes has been investigated.^{2–13} For

example; Yan and Lau² prepared polysulfone hollow-fiber ultrafiltration (UF) membranes with the dry/wet spinning process. With a mixture of water and *N*-1-methyl-2-pyrrolidone (NMP) in various proportions as the internal coagulant, the demixing rates of the polymer in the spinning solution can be adjusted to yield a more open surface structure in the fiber inner surface layer and a more porous sub-layer in the fiber wall to reduce the total transmembrane resistance. The rate of polymer demixing can be related to the difference between the solubility parameters ($\Delta\delta$) of the internal coagulant and that of the polymer. This difference can serve as a scale to indicate the coagulation power of the internal coagulant. At a low coagulation rate, fibers with a more open structure, both in the fiber wall and in its inner surface, can be made; these yield a higher membrane flux because of their lower transmembrane resistance.

Wang and coworkers^{3,4} fabricated poly(ether sulfone) (PES) and polysulfone asymmetric hollow-fiber membranes with excellent gas separation properties from spinning solutions containing PES, NMP/

Correspondence to: Q. F. Alsalhy (qusayalsalhy@uotechnology.edu.iq or qusayalsalhy@yahoo.com).

water, and NMP/ethanol solvent systems. They found that the use of internal coagulants, such as water, EtOH, *i*-PrOH, EtOH/water, and *i*-PrOH/water, with a moderate nonsolvent strength improved the hollow-fiber integrity and suppressed macrovoid formation.

Poly(vinylidene fluoride) (PVDF) hollow-fiber membranes were prepared by dry/wet and wet phase-inversion methods.^{5–8} The effects of water, ethanol, ethanol–water, dimethylacetamide, and *N,N*-dimethylacetamide (DMAc)–water and different ratios of NMP–water mixtures as internal coagulants on the structure and performance of the PVDF hollow fibers were studied. The examination of the membrane cross sections indicated that the composition of the internal coagulants had a significant impact on the thickness and morphology of the inner skin layer.

Also, UF hollow-fiber membranes of poly(acrylonitrile-*co*-maleic acid) (PANCMA) were prepared by a dry/wet phase-inversion process. The morphologies of the inner surface and cross section for these hollow fibers were analyzed with scanning electron microscopy (SEM). It was found that with an increase in the amount of the solvent dimethyl sulfoxide in the internal coagulant, the number and size of macrovoid underneath the inner surface decreased. The water flux of the hollow-fiber membranes also decreased, and the bovine serum albumin rejection increased minutely.⁹

Liu and Bai¹⁰ investigated the effects of chitosan (CS) and cellulose acetate (CA) concentrations in the spinning dope solutions and the compositions of the external and internal coagulants on the structures and morphologies of CS and CA blend hollow fibers as adsorptive membranes to achieve highly porous and macrovoid-free structures with different pore sizes. Water, a weaker coagulant, could be used as both an external and internal coagulant in the fabrication process, and the resultant CS/CA blend hollow fibers showed spongelike, macrovoid-free, and relatively uniform porous structures, which are desirable for adsorptive membranes.

The effects of DMAc as a solvent additive in bore fluid (BF) and acetic acid as a nonsolvent additive in dope solution on the morphologies and performances of poly(ether imide) (PEI) hollow-fiber UF membranes were investigated by Xu et al.¹¹ SEM studies indicated that the addition of DMAc to the internal coagulant changed the inner fiber surface from a dense skin layer to a porous structure, and the pure water flux of the membrane decreased with increasing DMAc content.

Polymeric solutions of a modified poly(ether ether ketone) and poly(vinyl pyrrolidone) (PVP) in dimethylformamide were spun to prepare hollow-fiber membranes by the dry/wet spinning method.¹² The influence of R–OH BFs with R=H, CH₃, C₂H₅,

n-C₃H₇, or *n*-C₄H₉ on the morphology, transport, and mechanical properties was studied by SEM and by measurements of water permeability, dextrane rejection, tensile strength, and elastic modulus. The results were discussed on the basis of ternary phase diagrams and Hildebrand solubility parameters (δ 's). The use of *n*-alkyl alcohols as BFs produced microfiltration (MF) membranes with water permeabilities increasing from about 600 to 1200 L h⁻¹ m⁻² bar⁻¹ with increasing alkyl chain length and with a low dextrane rejection.

In a previous work, the effects of the ethanol concentration in the internal coagulant on the morphology and separation performance of PES hollow-fiber UF membranes were investigated.¹³ It was found that the crack phenomenon appeared on the internal surfaces of the PES hollow-fiber membranes with increasing ethanol concentration from 60 to 100 wt % (pure ethanol). The pure water permeation fluxes (PWP) decreased from 39 to 23.3 (L/m² h bar), and the solute rejection increased with ethanol concentrations of less than 50 wt % in the internal coagulant. Then, PWP increased up to 65.4 (L/m² h bar), and the solute rejection decreased with additional increases in the ethanol concentration.

Xu and Xu¹⁴ prepared asymmetric poly(vinyl chloride) (PVC) hollow-fiber UF membranes by using PVP (molecular weight = 40,000) or poly(ethylene glycol) (PEG) with different molecular weights (600, 800, and 1000) as additives and DMAc as a solvent. It was found that the use of PVP or PEG as additives increased the PVC hollow-fiber porosity, enhanced the permeation flux, decreased the solute separation factor, and induced lower mechanical properties.

Khayet et al.¹⁵ prepared PVC hollow-fiber membranes by the dry/wet and wet/wet spinning techniques and investigated the effects of different air-gap distances on the morphology, properties, and UF performance of the produced fibers. They found that with increasing air-gap length, the fiber inner diameter (ID) and outer diameter (OD) decreased because of the gravitational force effect; the outer pore size and PWP both increased, whereas the solute separation factor decreased.

It is worth noting that to the authors' best knowledge, a systematic study of the solvent concentration effect of the internal coagulant on the morphological structure of the PVC hollow-fiber membranes had not yet been performed.

In this work, the effects of the DMAc concentration in the internal coagulant on the morphology, mechanical properties, and separation performances of PVC hollow-fiber membranes, fabricated with a dry/wet spinning technique, were investigated. The objective was to prepare PVC hollow fibers with different pore sizes for UF applications. The PVC

hollow fibers were characterized by their membrane void volume fraction (ϵ_m), $\Delta\delta$, pore size, pore size distribution, and SEM, whereas UF experiments were conducted with pure water and PVP K90 (code of the poly (vinyl pyrrolidone) (PVP) molecular weight in Sigma-Aldrich Chemical Company which is equal to 360000 KDa) as feeds.

EXPERIMENTAL

Materials

The hollow-fiber membrane material was PVC resin [weight-average molecular weight (M_w) = 65 kg/mol] with an average degree of polymerization of 1040 and obtained from Georgia Gulf Co. (Atlanta GA, USA). The solvent, *N,N* dimethyl acetamide (DMAc), was purchased from Sigma-Aldrich Chemical Co. PVP K90 (molecular weight = 360 KDa) was purchased from Sigma-Aldrich and was used for the preparation of the UF feed aqueous solutions.

Preparation of the PVC solution

To prepare the dope solution, PVC was dried overnight at 70°C. Solutions of PVC in DMAc were prepared by the mixture of the solvent and the polymer in a glass flask under magnetic stirring until the solution became homogeneous. The solution was then filtered on a 40- μ m stainless steel filter and left standing for at least 24 h to remove air bubbles. The PVC solution was then loaded in a vertical vessel with a 6 cm ID, and the temperature throughout the entire spinning run was 25°C.

PVC hollow-fiber spinning methods, apparatus, and posttreatment

The PVC hollow-fiber membranes were spun with the dry/wet spinning technique with various DMAc concentrations of the BF, from 0 to 80 wt %, and with all other spinning conditions kept constant. The spinneret used had an ID of 500 μ m and an OD of 900 μ m. The hollow-fiber PVC membranes were spun at room temperature with the dry/wet spinning method described elsewhere.^{16,17} Tables I and II summarize the composition and spinning conditions of the fabricated hollow-

TABLE I
Experimental Parameters Used in the Hollow-Fiber Spinning Process

Dope composition	15 : 85 (PVC/DMAc)
Extrusion pressure	0.75 (bar)
BF flow rate	6.65 (mL/min)
Air-gap distance	0.5 (cm)
External coagulant	Tap water
External coagulant temperature	Room temperature
Internal coagulant temperature	Room temperature
Spinneret dimensions	900/500 (OD/ID; μ m/ μ m)

TABLE II
Experimental Parameters of the Hollow-Fiber Spinning Experiments under Different Internal Coagulant Concentrations

Fiber no.	Dope composition		BF composition (wt %/wt %)
	Polymer (wt %)	Solvent (wt %)	
1	15	85	0.0–100 (DMAc/water)
2	15	85	40–60 (DMAc/water)
3	15	85	50–50 (DMAc/water)
4	15	85	60–40 (DMAc/water)
5	15	85	80–20 (DMAc/water)

fiber PVC membranes. The ratio of the dope flow rate to the BF flow rate was constant in all of the spinning processes. All nascent fibers were not drawn (no extension), which meant that the take-up velocity of the hollow-fiber membrane was nearly the same as the free-falling velocity in the coagulation bath. The coagulation bath and BF were both maintained at room temperature. The fabricated PVC hollow fibers were stored in a water bath for 24 h to remove the residual DMAc. Then, the fibers were kept in a 40 wt % glycerol aqueous solution for 48 h to prevent the collapse of porous structures and dried in air at room temperature before we prepared the membrane modules for the UF tests.

SEM observations

The membrane morphology was observed with a scanning electron microscope (Quanta FENG 200, FEI Co., Hillsboro, Oregon USA). The fiber cross sections were prepared by the freeze-fracturing of the samples in liquid nitrogen to produce clean brittle fractures. The internal and external surfaces were also observed.

$\Delta\delta$

δ 's of the solvents, nonsolvent, and PVC were obtained from Brandrup and Immergut's *Polymer Handbook*.¹⁸ The solubility parameter difference between PVC and a nonsolvent ($\Delta\delta_{P-NS}$) and the solubility parameter difference between a solvent and a nonsolvent ($\Delta\delta_{S-NS}$) could be calculated, respectively, from the following equations:

$$\Delta\delta_{P-NS} = \sqrt{(\delta_{d,P} - \delta_{d,NS})^2 + (\delta_{p,P} - \delta_{p,NS})^2 + (\delta_{h,P} - \delta_{h,NS})^2}$$

$$\Delta\delta_{S-NS} = \sqrt{(\delta_{d,S} - \delta_{d,NS})^2 + (\delta_{p,S} - \delta_{p,NS})^2 + (\delta_{h,S} - \delta_{h,NS})^2}$$

where the subscripts *d*, *P*, and *h* represent the dispersion, polar, and hydrogen-bonding components, respectively, of the δ of the pure component and the subscripts *S* and *NS* represent the solvent and nonsolvent, respectively.

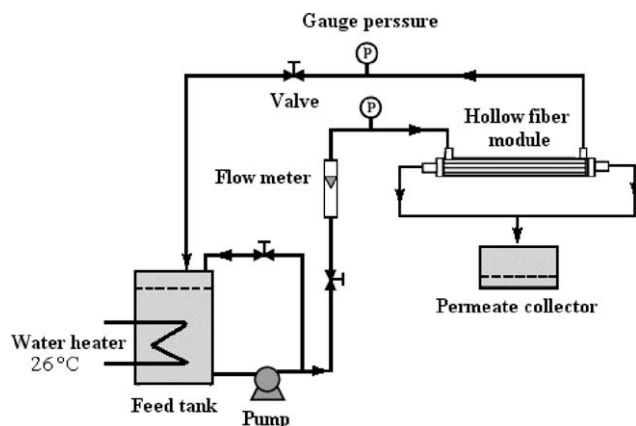


Figure 1 Schematic diagram of the UF experiments unit.

Mechanical properties

The tensile strengths of the fibers were measured by a Zwick/Roell (Ulm, Germany) Z 2.5 test unit. Each sample was stretched unidirectionally at a constant rate of 5 mm/min; the initial distance between the clamps was of 50 mm. Five specimens were tested for each sample. The breaking elongation and elastic or Young's modulus were determined.

Bubble point and average pore size measurements

A PMI capillary flow porometer (Porous Materials, Inc., Ithaca, NY USA) was used to measure the bubble point and the pore size distribution. The fibers were immersed in a porewick (surface tension = 16 dyne/cm) overnight to ensure complete wetting.

The measurements were based on Laplace's equation:

$$d_p = 4\gamma \cos \theta / P \quad (1)$$

where d_p is the pore size diameter, γ is the surface tension of the liquid, θ is the contact angle of the liquid, and P is the external pressure.

The fibers were analyzed with the wet-up/dry-up method. Capwin software was used to calculate the pore size distribution, which was exported as an Excel file with Caprep software (Porous Materials, Inc., Ithaca, NY USA).

ε_m measurements

ε_m can be defined as the volume of the pores divided by the total volume of the membrane. The overall porosity was calculated according to the following formula, as reported in the literature:¹⁹

$$\varepsilon_m = (1 - \rho_{\text{fiber}} / \rho_{\text{PVC}}) \quad (2)$$

where ρ_{fiber} is the fiber density and ρ_{PVC} is the PVC density (1.4 g/cm³).¹⁸

Measurements of the permeation flux and solute rejection

To quantitatively test the hollow-fiber separation performance in terms of the permeation flux and rejection, permeation modules were prepared. Each module consisted of five fibers with a length of 24 cm. The shell sides of the two ends of the bundles were glued into two stainless steel tees with a normal-setting epoxy resin. These modules were left overnight for curing before they were tested. To eliminate the effect of the residual glycerol on the module performance, each module was immersed in water for 1 day and run in the test system for 1.5 h before any sample collection.

Figure 1 shows a schematic diagram of the solute-water separation membrane unit. Experiments were carried out with hollow-fiber modules at a transmembrane pressure of 1 bar and at room temperature. Three modules were prepared for each hollow-fiber sample. The PWP's were obtained as follows:

$$J_w = \frac{V_w}{\Delta PS} \quad (3)$$

where J_w is the permeation flux of membrane (L m⁻²·h⁻¹·bar⁻¹), V_w is the volumetric flow rate (L/h), ΔP is the transmembrane pressure drop (bar), and S is the membrane surface area (m²). An aqueous solution of PVP (K90, $M_w = 360$ KDa) with a concentration of 1000 ppm was used for the measurement of solute rejection of each hollow-fiber module. The membrane rejection (R ; %) is defined as

$$R(\%) = \left[1 - \frac{C_p}{C_f} \right] \times 100 \quad (4)$$

where C_f and C_p are the solute concentrations in the feed and the permeate solution, respectively. The concentration of PVP was determined by the measurement of the optical density at a wavelength of 212 nm with an ultraviolet-visible spectrophotometer (Shimadzu UV160 A, Kyoto, Japan).

RESULTS AND DISCUSSION

Effect of the DMAc concentration in the internal coagulant on the structural morphology

As already reported in the Introduction, the internal coagulant plays an important role in the preparation of hollow-fiber membranes; it affects both the membrane morphology and the separation performance. In literature, there are several works that have already reported the internal coagulant composition effects on the structure and properties of polymeric hollow fibers²⁻¹³ but not with PVC as the polymer material.

Figure 2 shows SEM images of the cross-sectional structures of the PVC hollow-fiber membranes prepared with different DMAc concentrations as the internal coagulant (i.e., 0, 40, 50, 60, and 80 wt %). All of the PVC hollow fibers were composed of three layers; however, the membrane morphology was found to change when the DMAc concentration of the internal coagulant was varied from 0 to 80 wt %.

Figure 2(a) shows the cross section of one of the PVC hollow fiber prepared with pure water as the internal coagulant. It could be noticed that there was a small, fingerlike structural layer at the outer edge, whereas a large, fingerlike macrovoid layer, having a thickness equal to 58.5 μm , was situated at the middle of the cross section of the PVC hollow fiber. Thin, fingerlike macrovoids were noticed at the inner edge with a very small sponge structure situated between them. Although, with 40 and 50 wt % DMAc solutions as the internal coagulant, it could be seen that the thin, fingerlike structure at the inner edge became wider, and some sponge structure could be observed between them, as shown in Figure 2(b,c). A further increase in the DMAc concentration in the internal coagulant to 60 wt % changed the morphology of the layer near the inner edge of the PVC hollow fiber to a spongelike structure with small macrovoids concentrated near the inner edge, whereas the large, fingerlike macrovoids situated at the middle of the cross section extended toward the inner layer [Fig. 2(d)]. Figure 2(e) shows that with a DMAc concentration equal to 80 wt %, the configuration of the layer near the inner edge was fully changed to a spongelike structure, whereas under the inner skin layer, there were many circular macrovoids with a size of 1.9 μm , and a more extended layer (thickness = 98.47 μm) of large, fingerlike macrovoids was noticed toward the inner layer. The morphology of the layer near the inner edge of the PVC hollow fiber changed from a fingerlike to a spongelike structure with increasing DMAc concentration in the internal coagulant; this was attributed to the decrease of $\Delta\delta$ between PVC–nonsolvent and the solvent–nonsolvent, and strong interaction between the solvent and nonsolvent, which caused delayed nonsolvent penetration into the PVC solution, as shown in Table III.

For PVC, water is a strong nonsolvent, which means that coagulation occurs rapidly when the polymer solution is brought into contact with water. Several researchers have reported that during membrane coagulation, the strong interaction between the nonsolvent (water) and the solvents determines an instantaneous liquid–liquid demixing, which forms the fingerlike structure.^{1,16,20} Smolders et al.²¹ reasoned that under the top layer of the membrane, locally nuclei containing quite a high solvent concentration could be created, and as long as the solution remains stable, no new nuclei deeper in the mem-

brane could be formed, and the nucleus then could grow to form a fingerlike structure. However, the delayed liquid–liquid demixing in the membrane formation process happened using 80 wt % DMAc as the internal coagulant and resulted in a porous spongelike structure near the inner edge of the PVC hollow fibers.¹

Figure 3 shows the SEM images of the PVC hollow-fiber membrane internal surfaces prepared at different DMAc concentrations. The internal surface of the PVC hollow fibers spun with pure water as the BF had an open and large pore size with a low pore density [Fig. 3(a)]. Hollow-fiber membrane 2, coagulated with DMAc 40 wt %, showed a very thin skin covering large pores; in some regions, the skin was interrupted, and pores were open on the surface [Fig. 3(b)]. The internal surface of PVC fibers produced with DMAc 50 wt % as an internal coagulant, having large pores beneath the surface, was covered by a skin having a lacy structure [Fig. 3(c)]. In Figure 3(d), it can be noticed that fibers spun with DMAc 60 wt % as a BF exhibited very well-distributed interconnected pores. PVC hollow fibers produced with DMAc 80 wt % as the internal coagulant showed some valleys over the internal surface [Fig. 3(e)]. These were not true interconnected pores. In fact, as shown in Figure 2(e), the fiber inner layer had a closed-cell structure. As reported in the literature,²² when a strong coagulant, such as water, is used, it induces a rapid phase inversion in the nascent fiber and, consequently, leads to the formation of a dense skin. This can happen both at the inner and outer layer of the fiber and can lead to a low surface porosity. Mixtures of solvents and nonsolvents can be used as coagulants to induce a delayed demixing and, hence, to create a porous surface. Indeed, the morphology of the hollow-fiber membrane inner surface can be tailored by the adoption of a suitable composition of BF, such as a mixture of solvent and nonsolvent.

Figure 4 shows the SEM images of the external surfaces of PVC hollow fibers prepared under different DMAc concentrations in the internal coagulant. It can be seen that the external surface of the PVC hollow fiber looked dense, and no pores were observed, even at a high magnification (20,000 \times). This was in agreement with what was observed in literature.²² When water was used as the coagulation bath, a dense skin layer was formed because of the instantaneous liquid–liquid demixing process.

Effect of the DMAc concentration on the dimensions and ϵ_m

The internal and external diameters and the thickness of the PVC hollow fibers prepared under different DMAc concentrations in the internal coagulant

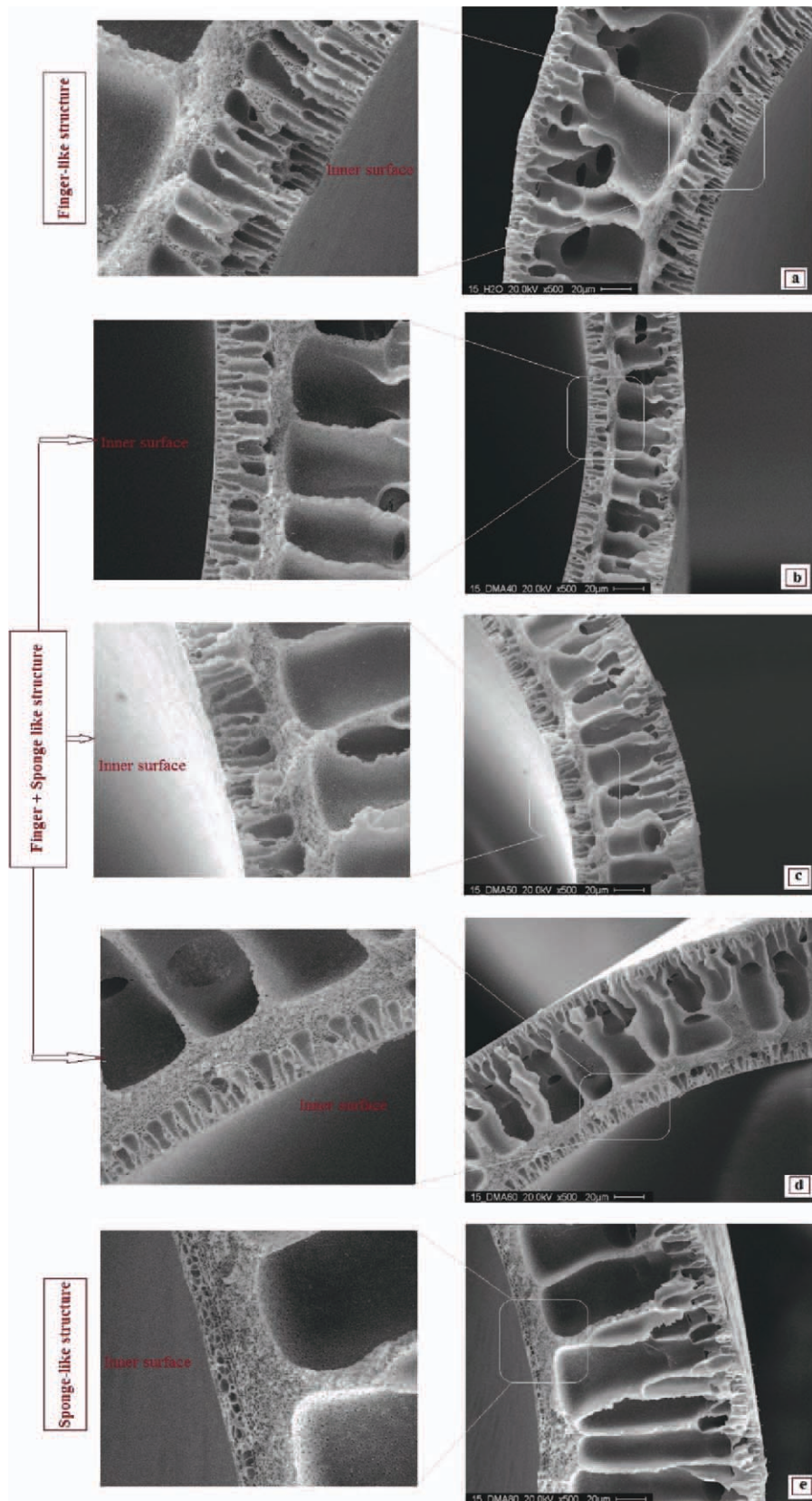


Figure 2 Cross-sectional structures of PVC hollow fibers prepared under different DMAC compositions in bore liquid (magnification = 500×): (a) 0, (b) 40, (c) 50, (d) 60, and (e) 80 wt % DMAC. [Color figure can be viewed in the online issue, which is available at wileyonlinelibrary.com.]

TABLE III
 δ 's and Their Differences [(MPa)^{1/2}]

Component	δ_d (MPa) ^{1/2}	δ_p (MPa) ^{1/2}	δ_h (MPa) ^{1/2}	$\Delta\delta_{P-S}$ (MPa) ^{1/2}	$\Delta\delta_{P-NS}$ (MPa) ^{1/2}	$\Delta\delta_{S-NS}$ (MPa) ^{1/2}
PVC	18.7	10.0	3.1			
Water	15.5	16.0	42.4			
DMAc	16.8	11.5	10.2			
DMAc/water (0 : 100)				7.501	39.884	32.539
DMAc/water (40 : 60)				7.501	14.78	7.374
DMAc/water (50 : 50)				7.501	12.67	5.25
DMAc/water (60 : 40)				7.501	11.164	3.735
DMAc/water (80 : 20)				7.501	8.97	1.513

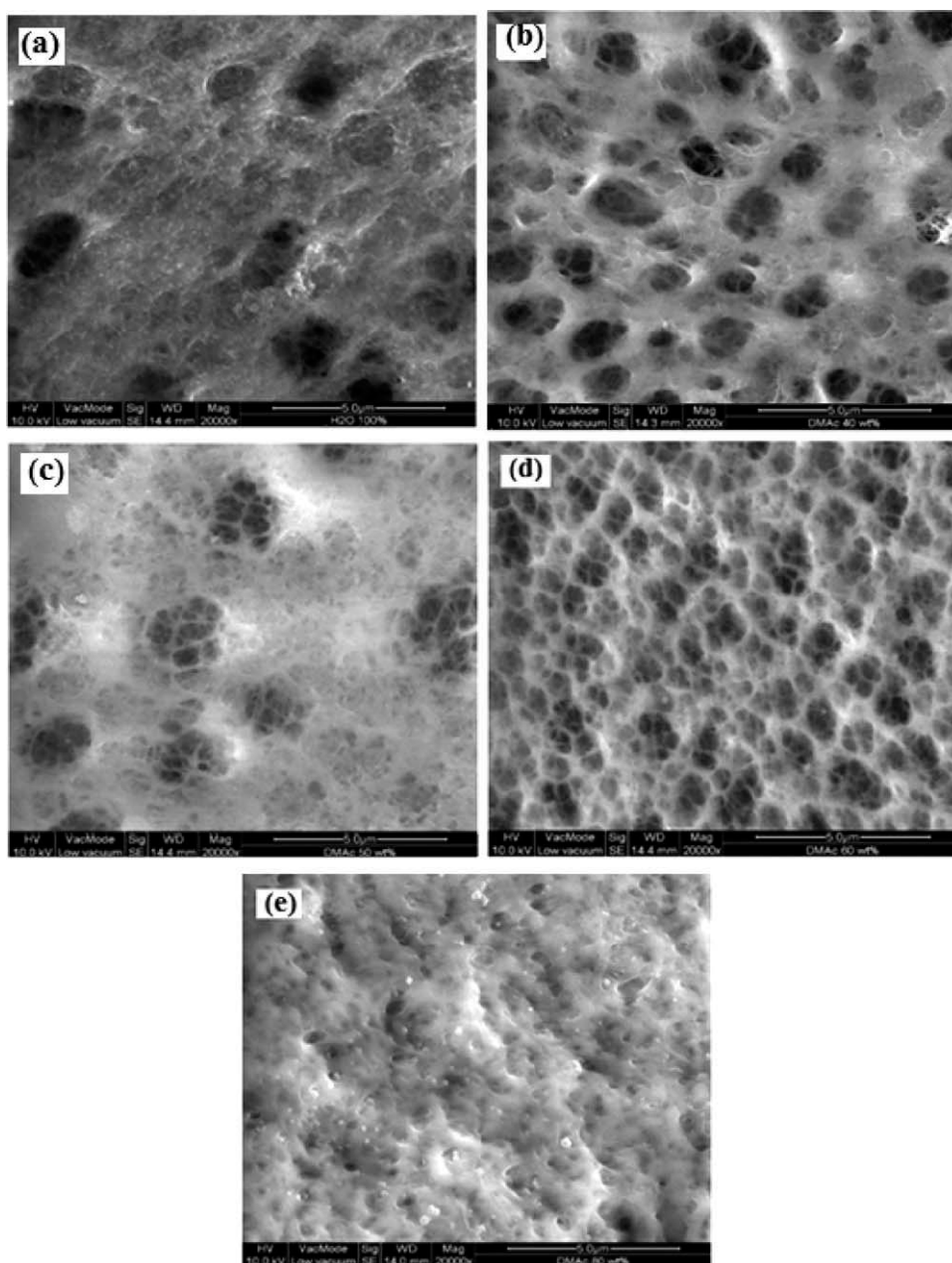


Figure 3 Internal surface structures of PVC hollow fibers prepared under different DMAC compositions in bore liquid (magnification = 20,000 \times): (a) 0, (b) 40, (c) 50, (d) 60, and (e) 80 wt % DMAC.

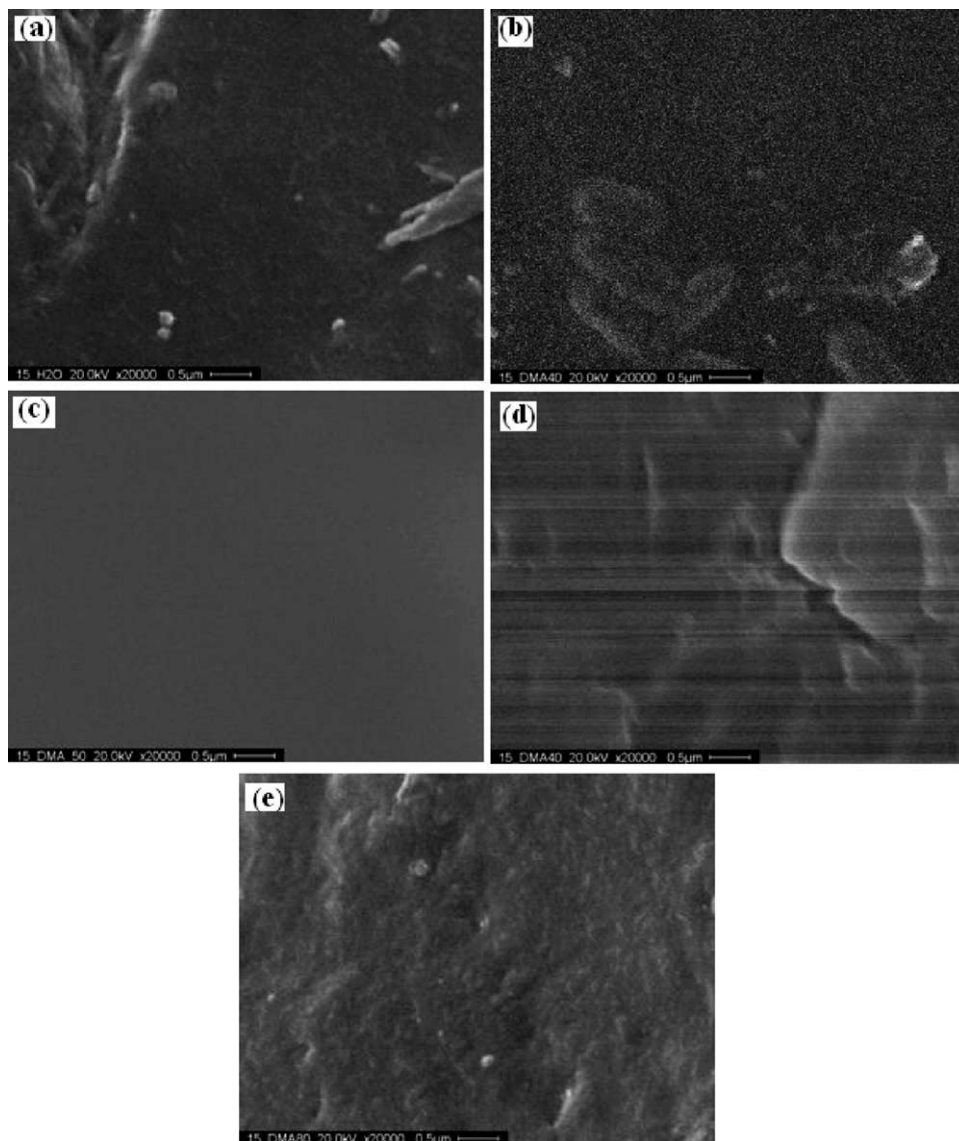


Figure 4 External surface structures of PVC hollow fibers prepared under different DMAc compositions in bore liquid (magnification = 20,000 \times): (a) 0, (b) 40, (c) 50, (d) 60, and (e) 80 wt % DMAc.

are summarized in Table IV. It can be seen that the internal diameters increased and the external diameters decreased with the increase in the DMAc concentration. The delayed liquid–liquid demixing process left the internal layer softer or not completely coagulated; this allowed the pressure of the bore liq-

uid to increase the diameter. When the coagulation was fast, the layer was formed immediately, and the internal diameter was immediately fixed. Tasselli et al.²³ ascribed this mainly to the inflation of the fiber caused by the much higher flow rate of the BF compared to that of the dope solution. The degree of

TABLE IV
Dimensions, Porosity, and Pore Density of the Dry-/Wet-Spun Fibers at Different DMAc Concentrations in the Internal Coagulant

Fiber no.	ID (mm)	OD (mm)	Membrane thickness (mm)	ϵ_m	Pore density (pores/cm ²)
1	0.683 \pm 0.014	1.011 \pm 0.019	0.164 \pm 0.004	0.620	4,487
2	0.725 \pm 0.016	1.084 \pm 0.037	0.180 \pm 0.022	0.608	^a
3	0.739 \pm 0.033	1.107 \pm 0.020	0.184 \pm 0.021	0.599	12,868
4	0.768 \pm 0.021	0.942 \pm 0.023	0.087 \pm 0.003	0.602	93,531
5	0.888 \pm 0.031	1.087 \pm 0.030	0.099 \pm 0.017	0.543	2,696

^a Not measured.

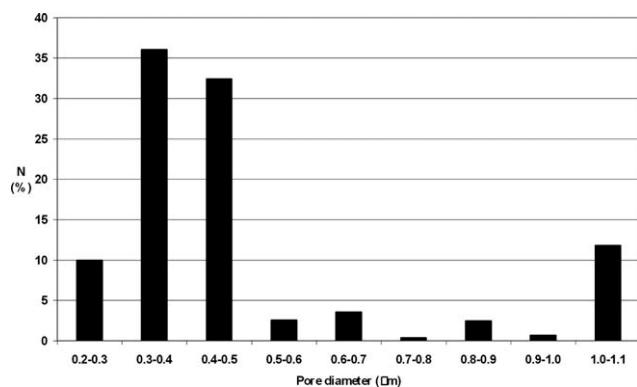


Figure 5 Pore size distribution of the PVC hollow-fiber membrane fabricated with 100 wt % pure water as an internal coagulant. [N (%) defined as the frequency of pores size].

inflation and, hence, the fiber dimensions depended on the internal coagulant composition through the mechanical strength of the forming fiber: a strong coagulant such as pure water instantaneously created a rigid polymer skin that was difficult to inflate, whereas a poor coagulant such as the 50/50 DMA/water mixture led to a delayed onset of liquid-liquid demixing and, hence, a slower gelation; this allowed a stronger inflation of the fiber.

The effect of the DMAc concentration as an internal coagulant on the ϵ_m (porosity) of the PVC hollow-fiber membranes is shown in Table IV. It was found that with an increase in the DMAc concentration from 0 to 80 wt %, ϵ_m diminished gradually from 0.62 to 0.54. This may have been due to the structural change of the hollow-fiber membrane from the fingerlike structure of the layer near the inner edge to a complete spongelike structure.

Effect of the DMAc in the internal coagulant on the pore size and pore size distribution

To improve the separation performance of the hollow-fiber membranes, the pore size and pores size

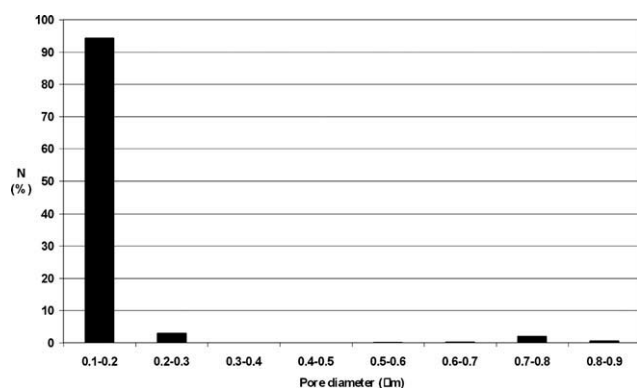


Figure 6 Pore size distribution of the PVC hollow-fiber membrane fabricated with 50 wt % DMAc as an internal coagulant. [N (%) defined as the frequency of pores size].

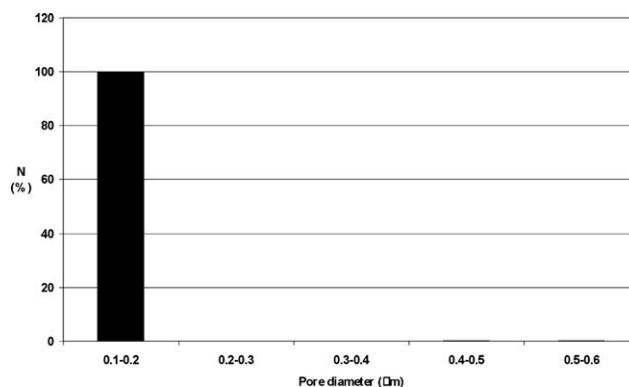


Figure 7 Pore size distribution of the PVC hollow-fiber membrane fabricated with 60 wt % DMAc as an internal coagulant. [N (%) defined as the frequency of pores size].

distribution needed to be controlled. Figures 5–8 show the influence of the DMAc concentration on the pore size and pore size distribution of the PVC hollow-fiber membranes prepared from PVC/DMAc (15 : 85) solutions. As shown in Figure 5, the effective pores showed a wide distribution between 0.2 and 1.1 μm for hollow fibers prepared with pure water as the internal coagulant. The frequency of pores having an average size of 0.235 μm was 10%; the one of 0.34- μm pores was over 35%, that of 0.44- μm pores was found to be over 32%, and that of the 1.1- μm pores was over 12%. The maximum pore size was 1.1 μm , as obtained from the bubble-point data. The pore density of this hollow-fiber membrane was also measured and was equal to 4487 pores/ cm^2 , as shown in Table IV. For hollow fibers prepared with 50 wt % in internal coagulant, the effective pores showed a narrow distribution, mainly between 0.1 and 0.2 μm , as shown in Figure 6. The maximum pore size was 0.868 μm , with a very low frequency (0.42%). The pore density of this hollow-fiber membrane was 12,868 pores/ cm^2 , as shown in Table IV. As shown in Figure 7, the effective pores showed a very narrow distribution, between 0.105 and 0.11

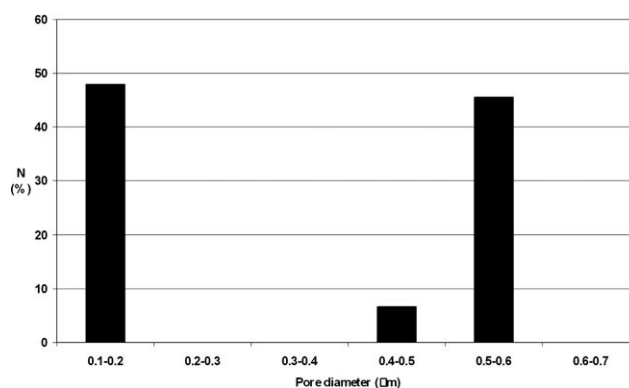


Figure 8 Pore size distribution of the PVC hollow-fiber membrane fabricated with 80 wt % DMAc as an internal coagulant. [N (%) defined as the frequency of pores size].

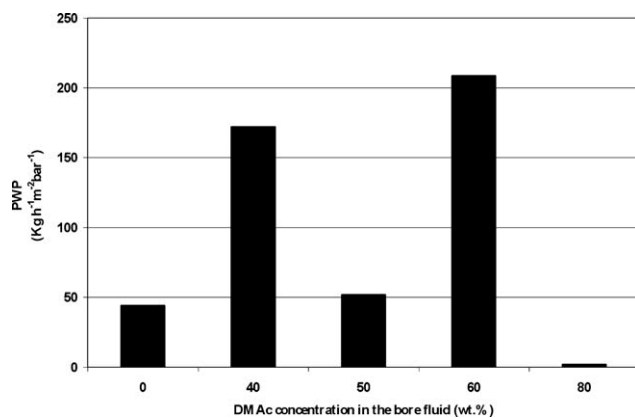


Figure 9 Effect of the DMAc concentration in the internal coagulant on the PWP.

μm , with a maximum pore size of $0.154 \mu\text{m}$ for hollow fibers prepared with a 60 wt % DMAc concentration in the internal coagulant. The pore density was equal to $93,531 \text{ pores/cm}^2$. Figure 8 shows the pore size distribution of the PVC hollow fibers prepared with an 80 wt % DMAc concentration in the internal coagulant. It can be seen that the effective pores showed a wide distribution, between 0.1 and $0.6 \mu\text{m}$. The maximum pore size was $0.557 \mu\text{m}$. The pore density of the PVC hollow-fiber membranes prepared with an 80 wt % DMAc concentration in the internal coagulant was 2696 pores/cm^2 . From the previous results, it could be observed that with increasing DMAc concentration in the internal coagulant, up to 60 wt %, the pore size decreased, and the pore size distribution become very narrow, with a high pore density on the surface of the PVC hollow-fiber membranes. This was due to a decrease in the $\Delta\delta_{P-NS}$ and the $\Delta\delta$ of DMAc and the nonsolvent, as shown in Table IV. In the case of the PVC system, the decrease in DMAc–nonsolvent $\Delta\delta$ led to a reduction in the diffusion of water into the inner surface of the PVC solution; therefore, it needed more time to complete the phase-inversion process of the membrane sublayers; this resulted in a delayed liquid–liquid demixing process. Chun et al.²⁴ reported that a lower pore size of membranes was observed for with decreasing $\Delta\delta_{P-NS}$ and the $\Delta\delta_{P-S}$. They explained the result by the diffusion exchange rate between the solvent and nonsolvent, the small $\Delta\delta_{S-NS}$ meant that the diffusion activation between the solvent and nonsolvent was not efficient because of the mass-transfer disturbance of the additive solvent. Hence, because of the addition of solvent to the coagulation bath, the $\Delta\delta_{S-NS}$ value was small, and delayed demixing occurs. Also, the addition of a greater amount of DMAc (i.e., 80 wt %) in the internal coagulant led to highly reduced pore density and the formation of a full spongelike structure at the inner edge of the PVC hollow fiber, as explained

earlier.¹¹ It was expected that the polymer solution would form a less porous membrane in coagulation baths with higher amounts of DMAc. This indicated that a very slow phase-inversion process happened between the PVC solutions and nonsolvents because of higher amounts of DMAc, and the sharp decline in ε_m of the PVC hollow fibers with 80 wt % DMAc in the internal coagulant shown in Table IV supported our expected. Thus, the physical and chemical properties of the internal fluid and those of the coagulation bath could have been a very important factor in the formation of the pore structure and the pore density.

Effect of the DMAc concentration in the internal coagulant on the hollow-fiber performance

Figures 9 and 10 show PWP and PVP K90 rejection of the PVC hollow-fiber membranes prepared with different DMAc concentrations in the internal coagulant. As shown in Figure 9, the pure water flux was in the following sequence: $80 < 0 < 50 < 40 < 60$ wt %. The rejection of PVP ($M_w = 360,000$) for the dry-/wet-spun PVC hollow fibers decreased from 95.6 to 60% with increasing DMAc concentration in the internal coagulant from 40 to 80 wt %, whereas the PVP rejection with pure water as the internal coagulant was 67.1%, as shown in Figure 10. In general, there are five major factors affecting hollow-fiber membrane performance: pore size, pore density, pore size distribution, porosity, and membrane thickness. In this work, the measured thickness of the PVC hollow-fiber membranes shown in Table IV did not follow the same trend as that observed for PWP and solute rejection compared with the other factors. This indicated that the pore size, pore size distribution, and pore density controlled the PVC hollow-fiber membrane performance, as shown in Figure 3 and Table IV. Therefore, the results could be explained by consideration of the pore size, pore

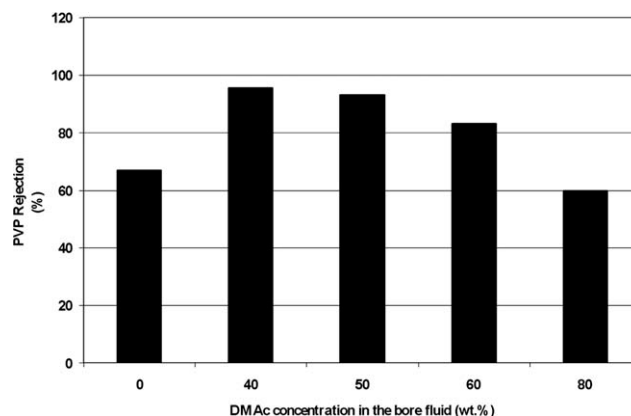


Figure 10 Effect of the DMAc concentration in the internal coagulant on the PVP rejection.

TABLE V
Hollow-Fiber UF Membrane Performance in Membranes Prepared from Different Membrane Materials in Terms of Total Pure Water Flux

Membrane material	Membrane configuration	Separation process	Pure water flux ($\text{l m}^{-2} \text{ h}^{-1} \text{ bar}^{-1}$)	Reference
PVDF	Hollow fiber	UF	152	6
PAN/CMA	Hollow fiber	UF	136	9
PEI	Hollow fiber	UF	23.41	11
Poly(ether ether ketone)	Hollow fiber	UF	158	12
PVC	Hollow fiber	UF	200	14
PES	Hollow fiber	UF	167	17
Poly(phthalazinone ether sulfone ketone)	Hollow fiber	UF	159	25
PES	Hollow fiber	UF	170	26
PVC	Hollow fiber	UF	209	This work

size distribution, and pore density of the produced PVC hollow-fiber membranes; this and the morphology of the fiber inner layer was described earlier. The fibers spun with pure water as the BF had a wide pore size distribution but a low pore density. As a result, the pure water permeability was low, and the rejection to PVP was low as well. Fibers spun with 50–60 wt % DMAc as the BF had a sharp pore size distribution; therefore, rejection improved. However, fibers spun with 60 wt % DMAc had a much higher pore density; as a consequence, the pure water permeability increased dramatically. Fibers spun with 80 wt % DMAc as the BF had a wider pore size distribution with respect to fibers produced with a lower DMAc concentration but a very low pore density and a closed-cell structure of the inner layer, as shown in Figures 2(e) and 3(e). As a result, both the rejection and the pure water permeability decreased. Xu and Alsahy¹⁷ reported that both PWP and the solute rejection were affected by the membrane pore size and pore density. The effect of the pore size on the solute rejection was obvious; solutes larger than the pore size were rejected, and smaller particles passed through the membrane surface. In practice, there was not a sharp distinction in size between the rejected particles and those that passed through the membrane surface. This reason was as follows. Membranes do not have pores of a single size; instead, there is a distribution of pore sizes, and for a particular particle, rejection will depend on whether it approaches a small or a large pore. However, even if the pores were of a uniform size, there would still not be a sharp cutoff, as hydrodynamic and shape effects would ensure that some particles, which are smaller than the pore size, would still be rejected by the membrane. This indicates that the solute transport may be governed by the respective pore size and pore size distribution, as explained in Figures 5–8.

To summarize, a comparison of the hollow-fiber UF membranes performance for the PVC membranes prepared in this work with selected literature values

for various membranes prepared from different polymeric materials is shown in Table V. It was observed that a hollow-fiber membrane prepared from PVC as a membrane material had a higher flux than most membranes.

With this method, PVC hollow-fiber membranes with a high PWP could be prepared, whereas the molecular weight cutoff of PVC hollow-fiber membranes was approximately 300,000. Because of the molecular weight cutoff of the UF membranes ranging from 1000–500,000, we concluded that this type of hollow fiber is suitable for UF applications.

Effect of the DMAc concentration in the internal coagulant on the mechanical properties

In industrial applications of membranes, the mechanical properties are very important for membrane performance. Therefore, the tensile strength and the elongation at break were measured and are shown in Table VI. The breaking load increased from 0.042 N m for the hollow fibers prepared from 60 wt % DMAc in the internal coagulant to 0.050 N m for the hollow fibers prepared from 40 wt % DMAc in the internal coagulant. Within experimental error, the tensile strength at break, the elongation at break, and the Young's modulus of the PVC hollow-fiber membranes seemed to be dependent on the DMAc concentration in the internal coagulant. As shown in Table VI, the elongation at break increased with increasing DMAc concentration in the internal coagulant, and the highest elongation at break was obtained for the hollow fibers prepared from 60 and 80 wt % DMAc concentrations (membranes 4 and 5). The tensile strength also increased with increasing DMAc concentration in the internal coagulant, and the highest tensile strength was obtained for the hollow fibers prepared from 80 wt % DMAc concentration in the internal coagulant (membrane 5). Also, the Young's modulus of the PVC hollow-fiber membranes increased with increasing DMAc concentration in the internal coagulant, and

TABLE VI
Mechanical Properties of the PVC Hollow-Fiber Membranes Spun from Different DMAc Concentrations in the Internal Coagulant

Fiber	Fiber breaking load (N m)	Fiber tensile strength (N/mm ²)	Fiber Young's modulus (N/mm ²)	Fiber breaking elongation (%)	σ_C (N/mm ²)
1	0.044 ± 0.005	2.380 ± 0.153	93.316 ± 5.312	57.600 ± 5.041	1.59
2	0.050 ± 0.000	2.720 ± 0.068	110.128 ± 5.354	62.275 ± 3.119	1.73
3	0.048 ± 0.004	2.570 ± 0.075	89.220 ± 3.571	71.828 ± 4.513	1.09
4	0.042 ± 0.004	1.978 ± 0.117	75.280 ± 6.348	83.778 ± 4.213	1.27
5	0.048 ± 0.012	3.962 ± 0.368	146.076 ± 14.135	69.940 ± 9.952	1.21

the highest value was obtained for the hollow fibers prepared with 80 wt % DMAc concentration (membrane 5). This could be attributed to the change in the fingerlike structure layer near the inner edge of the PVC hollow fibers to a spongelike structure with an increase in DMAc concentration in the internal coagulant. Tasselli and Drioli¹² reported that as the nonsolvent coagulant strength decreases, the slower phase inversion, in combination with the longitudinal stretching, allows a stronger orientation of the polymeric filaments before the final solidification of the coagulated polymer, and as a result, the modulus and tensile strength both increase. In addition, the mechanical properties depend on ε_m of the hollow fibers, increasing with decreasing ε_m of the hollow-fiber membranes. In agreement with our results, Xu and Xu¹⁴ reported that PVC hollow-fiber membranes with a lower porosity exhibited higher mechanical properties.

The fluid pressure was uniformly distributed over the inner surface of the hollow-fiber membrane, and it produced stress that acted tangentially to the circumference of the membrane. As a result of the transmembrane pressure exerted on the membrane wall, the maximum circumferential stress (σ_C) could be calculated from the following equation:

$$\sigma_C = \frac{(\text{TMP} \times \text{ID})}{2t} \quad (5)$$

where TMP is the transmembrane pressure exerted on the membrane

Therefore, taking into account the data reported in Table VI and the reported equation, we concluded that the operating pressure should not exceed 10 bar in all cases to protect fibers from rupture. It is worth mentioning that UF processes usually work under lower operating pressures. Hence, the produced fibers are suitable for use in UF.

CONCLUSIONS

PVC hollow fibers with different pore sizes for UF applications were successfully fabricated through a dry/wet spinning technique. The investigation was

conducted to evaluate the effects of different DMAc concentrations in the internal coagulant, and the following conclusions could be drawn:

1. The PVC hollow fibers were composed of three layers when the DMAc concentration in the internal coagulant was varied from 0 to 80 wt %. With an increase in the DMAc concentration in the internal coagulant from 0 to 80 wt %, the PVC hollow-fiber morphology changed slowly from a thin, fingerlike macrovoid structure formed at the inner edge to a fully spongelike structure because of the decreases of $\Delta\delta_{P-NS}$ and $\Delta\delta_{S-NS}$, and delayed demixing process occurs easier. There were many circular macrovoids, with a size equal to 1.9 μm , under the inner skin layer and a more extended layer of large, fingerlike macrovoids, with a thickness equal to 98.47 μm , toward the inner layer.
2. The internal diameters increased with higher DMAc concentration in the internal coagulant because of the delayed liquid-liquid demixing process, which left the internal layer softer or not completely coagulated and allowed the pressure of the bore liquid to increase the diameter.
3. ε_m decreased with DMAc concentration because of the structural change of the layer near the inner edge from fingerlike to completely spongelike.
4. The effective pores showed a better size distribution with higher pore size frequency and higher pore density for PVC hollow fibers prepared with a 60 wt % DMAc concentration in the internal coagulant with higher PWP.
5. The mechanical properties also depended on the DMAc concentration in the internal coagulant; both the tensile strength and the elongation at break tended to increase with increasing DMAc concentration. However, the highest Young's modulus was with PVC hollow fibers prepared under a 80 wt % DMAc concentration. This was attributed to the gradual change of the fingerlike structure layer near the inner edge of the PVC hollow fiber to a spongelike structure.

One of the authors (Q.F.A.) gratefully thanks the Institute on Membrane Technology, Institute on Membrane Technology, National Research Council, and the Department of Chemical Engineering and Materials, University of Calabria, Rende, Italy, for the characterization of the produced fibers. Mariano Davoli (Department of Earth Science, University of Calabria) is also gratefully acknowledged for the use of the scanning electron microscope.

References

1. Kesting, R. E. *Synthetic Polymeric Membranes: A Structure Perspective*, 2nd ed.; Wiley: New York, 1985.
2. Yan, J.; Lau, W. W. Y. *Sep Sci Technol* 1998, 33, 33.
3. Wang, D.; Li, K.; Teo, W. K. *J Membr Sci* 2000, 176, 147.
4. Wang, D.; Teo, W. K.; Li, K. *J Membr Sci* 2002, 204, 247.
5. Wang, D.; Li, K.; Teo, W. K. *J Membr Sci* 2000, 178, 13.
6. Wang, D.; Li, K.; Teo, W. K. *J Membr Sci* 1999, 163, 211.
7. Yeow, M. L.; Yutie Liu, K. L. *J Membr Sci* 2005, 258, 16.
8. Xu, A.; Yang, A.; Young, S.; deMontigny, D.; Tontiwachwuthikul, P. *J Membr Sci* 2008, 311, 153.
9. Nie, F.-Q.; Xu, Z.-K.; Ming, Y.-Q.; Kou, R.-Q.; Liu, Z.-M.; Wang, S.-Y. *Desalination* 2004, 160, 43.
10. Liu, C.; Bai, R. *J Membr Sci* 2006, 279, 336.
11. Xu, Z.-K.; Shen, L.-Q.; Yang, Q.; Liu, F.; Wang, S.-Y.; Xu, Y.-Y. *J Membr Sci* 2003, 223, 105.
12. Tasselli, F.; Drioli, E. *J Membr Sci* 2007, 301, 11.
13. Alsalhy, Q. *Eng Technol J (Univ Technol—Baghdad)* 2007, 25, 253.
14. Xu, J.; Xu, Z. L. *J Membr Sci* 2002, 208, 203.
15. Khayet, M.; García-Payo, M. C.; Qusay, F. A.; Zubaidy, M. A. *J Membr Sci* 2009, 330, 30.
16. Xu, Z. L.; Alsalhy, Q. *J Appl Polym Sci* 2004, 91, 3398.
17. Xu, Z. L.; Alsalhy, Q. *J Membr Sci* 2004, 233, 101.
18. Brandrup, J.; Immergut, E. H. *Polymer Handbook*, 3rd ed.; Wiley: New York, 1989.
19. Wang, K. Y.; Chung, T. S.; Gryta, M. *Chem Eng Sci* 2008, 63, 2587.
20. Strathmann, H.; Kock, K.; Amar, P. *Desalination* 1975, 16, 179.
21. Smolders, C. A.; Reuvers, A. J.; Boom, R. M. *J Membr Sci* 1992, 73, 259.
22. Bonyad, S. I.; Chung, T. *J Membr Sci* 2009, 331, 66.
23. Tasselli, F.; Jansen, J. C.; Drioli, E. *J Appl Polym Sci* 2004, 91, 841.
24. Chun, K.-Y.; Jang, S.-H.; Kim, H.-S.; Kim, Y.-W.; Han, H.-S.; Joe, Y.-I. *J Membr Sci* 2000, 169, 197.
25. Yang, Y. Q.; Yang, D.; Zhang, S.; Wang, J.; Jian, X. *J Membr Sci* 2006, 280, 957.
26. Ç, P. Z.; Rolevink, E.; van Rijn, C.; Lammertink, R. G. H.; Wessling, M. *J Membr Sci* 2010, 347, 32.